NUMERICAL ANALYSIS OF BUOYANCY IN MIXED CONVECTION HEAT TRANSFER IN LID-DRIVEN CAVITY FLOWS

Dionísio Carmignan Neto, neto.mecanica@yahoo.com.br
Elizaldo Domingues dos Santos, edsantos@mecanica.ufrgs.br
Francis Henrique Ramos França, frfranca@mecanica.ufrgs.br
Adriane Prisco Petry, adrianep@mecanica.ufrgs.br
Department of Mechanical Engineering
Universidade Federal do Rio Grande do Sul – Rua Sarmento Leite, 425 – Porto Alegre - RS

Abstract. *The present work aims at evaluating the influence of several buoyancy forces on the fluid dynamics and thermal behavior of transient, two-dimensional lid-driven cavity flows with mixed convection heat transfer. In order to achieve this purpose, several flows with stable and unstable stratification for the Richardson numbers of Ri = 0.0 (forced convection), 0.1, 0.25, 0.5, 0.75, 1.0, 2.5, 5.0, 7.5 and 10.0 are simulated. For all performed simulations the Reynolds and Prandtl numbers are kept fixed, Re_H = 400 and Pr = 6. The conservation equations of mass, momentum and energy are solved using a commercial code based on the finite volume method (FLUENT®). The transient velocities and temperature fields obtained from the present code for the stable stratification flow (Re_H = 400, Pr = 6 and Ri = 0.1) are compared with the ones presented in the literature, showing an agreement within 6%. The results for local Nusselt number on the lower and upper surface of the cavity are obtained as a function of the Richardson number. For simulations with stable stratification, the increase of the Richardson number significantly suppressed the main vortex formation resulting in a strong decrease of the local Nusselt number magnitude. For the cases with unstable stratification, the increase of the Richardson number has the opposite effect. The increase of the Richardson number for this kind of stratification also modifies the fluid dynamic and thermal behavior of the flow, intensifying the mixture between hotter and colder portions of fluid. This fact is reflected over the local Nusselt number, especially for Ri = 10.0. For this case, it is also noticed the arising of secondary vortices in the upstream lower region of the cavity. Moreover, the space averaged Nusselt number is obtained and these results led to the observation that stable stratification has a higher influence over flows where the fluid dynamic and thermal behavior are dominated by inertial forces, while unstable stratified flows has a higher influence over flows where the buoyancy effect is dominant. Additionaly, the increase of the Richardson number increases the difference between the space averaged Nusselt number reached for flows with unstable and stable stratification. The minimum difference, obtained for Ri = 0.1, is approximatelly 14%, while the maximum difference, for Ri = 10.0, is almost 94%.*

Keywords*: Mixed Convection, Cavity Flows, Laminar Flow, Richardson Numbers.*

1. INTRODUCTION

Cavities represent a geometrical idealization for various engineering fluid flows. Some examples include interstitial flows between fins in heat exchangers, systems for storage of solar energy and the space among electronic components in an integrated board. The main advantages for the study of cavities is its simple geometry, well posed boundary conditions and the presence of complex phenomena such as the boundary detachment and reattachment and the generation of primary and secondary vortices. In this sense, several studies have been carried out aiming at understanding the fluid dynamic and thermal behavior of internal flows (Prasad and Koseff, 1989; Prasad and Koseff, 1996).

For isothermal flows, various studies in cavity flows has been reported in the literature employing the experimental and numerical approaches with the objective to better understand the fluid dynamics of laminar (Guia *et al.*, 1982; Prasad and Koseff, 1989) and turbulent internal flows (Prasad and Koseff, 1989; Kim and Menon, 1999). For forced convection cavity flows, some studies in laminar and high Reynolds numbers flows were carried out aiming at understanding the influence of the fluid dynamics over the energy transport for internal flows (Nallasamy and Prasad, 1977; Dos Santos *et al.*, 2008).

Concerning the study of mixed convection heat transfer in cavity flows, it is worthy to mention the experimental work of Prasad and Koseff (1996), where it is evaluated the influence of different Reynolds and Richardson numbers ($0 \leq Re \leq 12000$ and $0.1 \leq Ri \leq 1000$) over the fluid dynamic and thermal behavior of unstable stratified cavity flows. Other important studies are performed in the numerical field with the purpose to investigate mixed convection in laminar cavities flows. For instance, Iwatsu and Hyun (1995) investigated the effect of external excitation in the structure of the flow with stable stratification in a square cross-section cavity, and verified the influence of the dimensionless groups (Re and Ri) in the formation of three-dimensional structures, such as the Taylor-Göertler vortex. Mohamad and Viskanta (1995) analyzed flows with stable stratification in cavities, aiming at verifying the influence of the slipping in the thermal field for shallow cavities. Khanafer et al. (2007) performed a numerical study in cavities in the transient regime, investigating the effect of the sliding top plate, which was submitted to a sinusoidal, horizontal

oscillation. In addition, an experimental and numerical study was presented in Ji *et al.* (2007) for transient flows in cavities with mixed convection and stable stratification for a wide range of Reynolds and Grashoff numbers: $400 \leq Re \leq 4\,000$ and $1.6\times10^5 \leq Gr \leq 1.6\times10^7$. However, at the authors knowledge, few has been presented about the influence of the kind of stratification for several values of Richardson numbers over the transient thermal behavior and the heat transfer in cavity surfaces.

The main goal of the present work is to evaluate the influence of the kind of stratification (stable/unstable) for several Richardson numbers (Ri = 0.0, 0.1, 0.25, 0.5, 0.75, 1.0, 2.5, 5.0, 7.5 and 10.0) over the transient fluid dynamic and thermal behavior of laminar flows. Moreover, it is numerically investigated the influence of these parameters over the heat transfer process at cavity surfaces (Nusselt number). The choice of the Richardson numbers is based on the previous findings of Mohamad and Viskanta (1995) and Ji *et al.* (2007) which observed that for mixed convection flows there is an equilibrium between inertial and buoyancy forces for Richardson numbers of the order of unity ($Ri \approx 1$) and a inertial and buoyancy dominance for Richardson numbers lower and higher than this order, respectively. For all performed simulations the Reynolds and Prandtl numbers are kept fixed, $Re_H = 400$ and $Pr = 6$. The simulations of the present work are performed with the use of a CFD code based on rectangular finite volume (Fluent, 2007).

2. MATHEMATICAL AND NUMERICAL MODELING

The modeling of transient, non-isothermal flows is based on the solution of conservation equations together with the boundary and the initial conditions. The conservation equations of mass, momentum and energy, valid in an orthonormal basis, are given by (Bejan, 2004):

$$\frac{D\rho}{Dt}+\rho\frac{\partial v_j}{\partial x_j}=0 \qquad (j = 1, 2 \text{ and } 3) \text{ in } t\times\Omega \tag{1}$$

$$\frac{\partial}{\partial t}(\rho v_i)+\frac{\partial}{\partial x_j}(\rho v_i v_j)+\frac{\partial P}{\partial x_j}\delta_{ij}-\frac{\partial}{\partial x_j}\left\{\rho\upsilon\left(\frac{\partial v_i}{\partial x_j}+\frac{\partial v_j}{\partial x_i}\right)+\lambda\frac{\partial v_k}{\partial x_k}\right\}+\rho g_i\beta(T-T_0)=0 \qquad (i, j, k = 1,2 \text{ and } 3) \text{ in } t\times\Omega \tag{2}$$

$$\frac{\partial T}{\partial t}+\frac{\partial}{\partial x_j}(v_j T)-\frac{\partial}{\partial x_j}\left\{\alpha\frac{\partial T}{\partial x_j}\right\}-q'''=0 \qquad (j =1,2 \text{ and } 3) \text{ in } t\times\Omega \tag{3}$$

where ρ is the specific mass of the fluid (kg/m³); β is the thermal expansion coefficient (K^{-1}); C is the sound propagation speed (m/s); μ is the dynamic viscosity (kg/ms); λ is the volumetric viscosity (kg/ms); υ is the kinematic viscosity (m²/s); α is the thermal diffusivity (m²/s); v_i is the velocity in i-direction, i = 1, 2 and 3 (m/s); x_i corresponds to the spatial coordinate, i = 1, 2 and 3 (m); P is the pressure (N/m²); T is the temperature (°C or K); T_0 is the reference temperature (°C or K); g_i is the gravity acceleration in i-direction, i = 1, 2 and 3 (m/s²); δ_{ij} is the Kronecker delta; Ω is the spatial domain (m); t represents the time domain (s) and q''' is the heat source term (W/m³) and D()/Dt is the substantial derivate.

Equation (1)-(3) are solved by using a CFD package based on rectangular finite volume (Fluent, 2007). The solver is pressure based, the velocity-pressure coupling is performed with SIMPLE method and for the treatment of advective dominant flows is employed the Second Order Upwind for momentum equations and Power-Law for the energy equation. More details concerned with the finite volume method can be found in Versteeg and Malalasekera (1999), Maliska (2004) and Patankar (1980).

The grid independence for each flow is achieved when the relative deviation between the average profiles of velocity and temperature obtained for two grids are less than 0.1%. To establish the grid independence the following grids were compared: 40×40, 60×60, 80×80, 100×100 and 120×120. The independent grid reached was 100×100. All the results were obtained for an instant of time of 4.40×10^{-2} s.

3. DESCRIPTION OF THE PROBLEM

The analyses of the present problem consider two-dimensional cavities with square cross-section. The sole difference between the simulations with stable and unstable stratification is the prescription of the higher temperature on the upper or lower surfaces, respectively, as can be seen in Fig. 1(a) and 1(b). The fluid flow in the cavity is generated by the motion of an infinite plate that also represents the upper surface (xz plane). The velocity of the plate is taken as the reference velocity for the computation of the Reynolds number. In addition, this surface presents the non-slip and the impermeability boundary conditions. For the lateral and lower surfaces, the dimensionless velocities are prescribed as null ($v_1^* = v_2^* = 0$). As for the thermal field, the heating of the fluid is a result of imposing a dimensionless temperature of $T^* = 1$ on the upper surface for the case of stable stratification and on the lower surface for the unstable stratification, where the temperature of the other surface (lower and upper surfaces, respectively) is prescribed as $T^* = 0$.

The lateral surfaces are treated as adiabatic. The velocities and temperatures at the cavity corners are assumed the same of the superior and inferior surfaces. The dimensionless terms, represented by the superscript *, are defined as:

$$x_i^* = \frac{x_i}{H} \qquad \text{(i =1, 2 and 3)} \tag{4}$$

$$v_i^* = \frac{v_i}{v_{1\max}} \qquad \text{(i =1, 2 and 3)} \tag{5}$$

$$T^* = \frac{(T - T_{\inf})}{(T_{\sup} - T_{\inf})} \tag{6}$$

where H is the height of the cavity; $v_{1\max}$ is the sliding velocity of the top surface; and $T_{\sup}$ and $T_{\inf}$ are the largest and the smallest temperatures in the cavity.

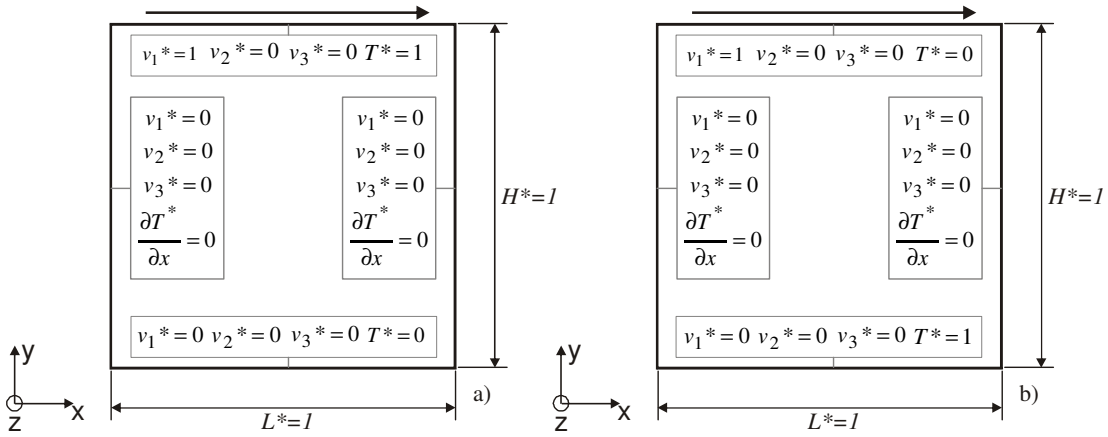

Figure 1. Cavity flow domain: (a) stable stratification, (b) unstable stratification.

For the initial conditions, it is considered that the fluid is still, with null velocities and pressure in the entire domain, and with a stratified temperature field, defined by a linear function along the dimensionless coordinate y^*, that is, temperature varying linearly from the lower surface to the upper surface.

The dimensionless time is defined by:

$$t^* = \frac{t v_{1\max}}{H} \tag{7}$$

In this study, the fluid flows were simulated for the following range of the governing dimensionless groups: Re_H = 400, $1.6 \times 10^4 \leq Gr_H \leq 1.6 \times 10^6$, $0.1 \leq Ri \leq 10.0$, and $Pr = 6$, where the Reynolds number is $Re_H = \rho v_{1\max} H/\mu$, the Grashoff number $Gr_H = g\beta\Delta T H^3/\upsilon^2$ and the Richardson number is $Ri = Gr/Re^2$.

4. RESULTS AND DISCUSSION

For validation of the code it was simulated a transient, incompressible, laminar, mixed convection flow at Re_H = 400, Pr = 6 and Ri = 0.1. For this analysis a numerical verification point was placed in the position x^*= 0.5 and y^*= 0.27 with the purpose to evaluate the time evolution of dimensionless velocity in x^*-direction (v_1^*) and temperature (T^*). The results obtained in the present code were compared with numerical simulations of Ji *et al.* (2007) and Dos Santos *et al.* (2009). Figure 2a shows the time evolution of dimensionless velocity in x^*-direction. As can be seen, the results obtained in the present work for the velocity fields were in close agreement with those presented in the literature, especially the ones of Ji *et al.* (2007), which used the same methodology for solving the conservation equations of mass, momentum and energy (finite volume method). Concerning the temperature fields, the difference between the results obtained in the present work and those presented by Ji *et al.* (2007) were negligible. In a comparison with the results of Dos Santos *et al.* (2009), few differences were observed in the range $6 \leq t^* \leq 10$. In the worst situation a percentual deviation was lower than 6%. Other numerical points were inserted in the following placements: x^*=0.5, y^*=0.48 and x^*=0.5, y^*=0.93. The deviation between the velocity and temperature fields as a function of time for these placements was lower than that presented for x^*=0.5, y^*=0.27 and, for the sake of brevity, will not be presented here.

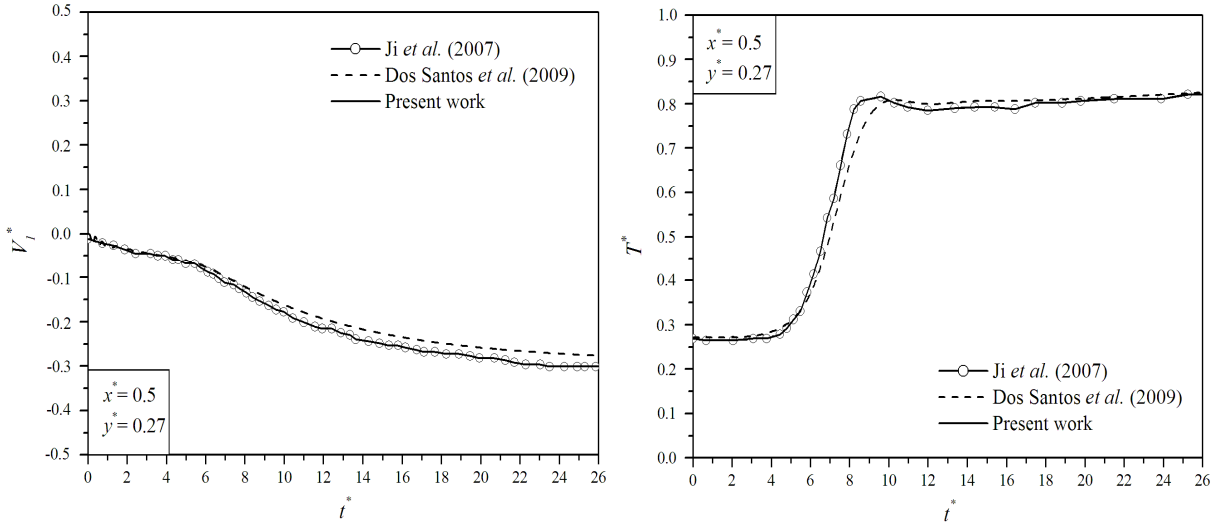

Figure 2. Comparison of the transient behavior obtained in the present work with those presented in the literature: (a) velocity field, (b) temperature field.

Figure 3 presents the time evolution of the temperature field for the flow with Re_H = 400, Pr = 6 and Ri = 0.1 and two kinds of stratification: stable and unstable. The steps in the dimensionless temperature are of $\Delta T^* = 0.1$. In the present simulations it is evaluated the influence of the kind of stratification for flows with dominance of inertial forces. Figures 3a - 3d show the topologies of the temperature fields for the following dimensionless times: $t^* = 1.4$, $t^* = 3.7$, $t^* = 5.0$ and $t^* = 100.0$ (steady state), respectively, for the stable stratified flow. Figures 3e - 3h exhibit the topologies of the temperature fields for the unstable stratified flow at the same times than those presented for stable stratified flow.

As seen in Fig. 3a and 3e, for time step of $t^* = 1.4$, it was noticed the initial formation of the main vortex in the top right region of the cavity. For both simulations, stable and unstable, the physical mechanism responsible by the main vortex generation was the same, i.e., the formation of a mixture layer due to the velocity difference generated by the imposition of the displacement of the upper infinite plate. As time advances, the Kelvin-Helmholtz instabilities in the interface between two adjacent layers of the fluid developed into spiral shaped vortices for both stratifications, as seen in Fig. 3b and 3f for $t^* = 3.7$. Afterwards, for the time step of $t^* = 5.0$, it was already possible to see that the main vortex had a higher penetration towards the lower region of the cavity for the unstable stratified flow in comparison with the stable one, since for the latter case the cold fluid placed on the lower region of the cavity inhibited the development of the main vortex toward the center of the cavity. Figures 3d and 3h show the temperature topologies at a time step $t^* = 100.0$ (steady state) for the stable and unstable stratification flows, respectively. In general, the behavior of the temperature topologies had a similar behavior for both cases at the steady state. Nevertheless, for the case with unstable stratification the temperature field seems more affected by the mixture between colder and hotter portions of fluid. This was evidenced in the lower surface of the cavity and in the downstream corner of the cavity, where the temperature gradients were more intense for the flow with unstable stratification.

Figure 4 presents the time evolution of the temperature field for the flow with Re_H = 400, Pr = 6 and Ri = 1.0 and two kinds of stratification: stable and unstable. The steps in the dimensionless temperature are of $\Delta T^* = 0.1$. Here is evaluated the effect of the augmentation of the Richardson number, until the order of equilibrium between inertia and buoyancy forces, for both stratification over the transient behavior of the temperature field. Figures 4a - 4d show the topologies of the temperature fields for the following dimensionless times: $t^* = 1.8$, $t^* = 4.1$, $t^* = 6.9$ and $t^* = 100.0$ (steady state), respectively, for the stable stratified flow. Figures 4e - 4h exhibit the topologies of the temperature fields for the unstable stratified flow at the same times employed for the evaluation of the stable stratified flow.

For the time step of $t^* = 1.8$, Fig. 4a and 4e, one observes a similar behavior than those predicted for the initial time step with Ri = 0.1. In the beginning of the simulation, it was already possible to notice that the detachment of the cold fluid from the upper surface for the unstable stratified flow was more intense than the detachment of the hot fluid from the upper surface for the case with stable stratification. For the time step $t^* = 4.1$, it was observed the effect of the stratification over the behavior of the temperature field. For the stable stratified flow, the main vortex was suppressed in the upper region of the cavity due to the placement of the colder portion of the fluid in the lower region of the cavity, inhibiting the displacement of the main vortex toward the center of the cavity. On the contrary, the cold portion of fluid localized in the main vortex region detached from the upper surface of the cavity and it moved towards the lower surface, i.e., the unstable stratification facilitated the penetration of the main vortex inside the cavity. Besides that, higher temperature portions of fluid were displaced from the lower cavity regions towards the upper surface, creating a kind of jet in the region adjacent to the upstream cavity surface. It is also worthy to mention that the mixture of hotter

and colder temperatures was intensified for the case with unstable stratification. Afterwards, for the time step of $t^* = 6.9$, the stable stratification (Fig. 4c) imposed a restriction to the main vortex that continues suppressed in the upper region of the cavity and only some instabilities of Kelvin-Helmholtz were generated in the lower region of the cavity. On the contrary, for the unstable stratified simulation, Fig. 4g, the fluid was intensively mixed and the main vortex occupied almost the entire cavity. It was also observed in the former case, the formation of a secondary vortex near the downstream lower corner. For the steady state, the behavior of the temperature topologies was different for the two kinds of stratification, Fig. 4d and 4h. For the stable stratified flow, the heat transfer in the lower region of the cavity occurred almost exclusively by diffusion, while for the unstable flow the mixture intensified the temperature gradients near the lower surface. Moreover, it was observed two recirculations: the first one was the main vortex imposed by the displacement of the upper surface and other one was a minor recirculation placed in the lower region of the cavity. It was also noticed that the unstable stratified flow behaved periodically in time, which not occurred for the case with stable stratification.

Figure 5 presents the time evolution of the temperature field for the flow with $Re_H = 400$, $Pr = 6$ and $Ri = 10.0$ and two kinds of stratification: stable and unstable. The steps in the dimensionless temperature are of $\Delta T^* = 0.1$. The present simulations are employed for the evaluation of the effect of the kind of stratification over the flows which are dominated by buoyancy forces. Figures 5a - 5d show the topologies of the temperature fields for the following dimensionless times: $t^* = 0.5$, $t^* = 1.15$, $t^* = 1.95$ and $t^* = 100.0$ (steady state), respectively, for the stable stratified flow. Figures 5e - 5h exhibit the topologies of the temperature fields for the unstable stratified flow at the same times employed for the evaluation of the stable stratified flow.

For the case with stable stratification, one observes in Fig. 5a the formation of Kelvin-Helmholtz instabilities for $t^* = 0.5$. Afterwards, for the subsequent time steps ($t^* = 1.15$ and $t^* = 1.95$) the main recirculation continued restricted to the upper region of the cavity. At the steady state, it was observed that the increase of the Richardson number smoothed the mixture process. Additionally, the heat transfer process at the lower surface was dominated by diffusion. This behavior is in agreement with the previous findings of Iwatsu and Hyun (1995), Ji *et al.* (2007) and Mohamad and Viskanta (1995). For the unstable stratified flow, it was observed that, for the initial time step of $t^* = 0.5$, Fig. 5e, the generation of Kelvin-Helmholtz instabilities occurred similarly to the flow with stable stratification, showing that the formation of these structures is concerned with the same physical mechanism, i.e., the displacement of the upper surface. For the time step of $t^* = 1.15$, Fig. 5f, the cold mass of fluid detached from the upper surface, even before the formation of Kelvin-Helmholtz vortex. Afterwards, it was observed the displacement of the cold mass of fluid towards the lower region of the cavity. This displacement happened significantly due to the difference of density between the coldest and hottest portion of the fluid. The effect of buoyancy was also evidenced by the displacement of the higher temperature portions of fluid from the lower to the upper surface of the cavity, which happened close the upstream surface. Besides that, it was observed the generation of secondary vortices in the lower region of the cavity. At the steady state, Fig. 5h, it was observed that the mixture process was more intense than the previous case, $Ri = 0.1$, due to the increase of buoyancy forces. It was also noticed in Figure 5h that the main vortex penetrated inside the cavity more than the case with unstable stratification and $Ri = 0.1$. Besides that, the imposition of the main vortex associated with the buoyancy forces caused the generation of secondary vortices near the upstream and downstream lower corners, which can generate peaks of heat transfer in these regions.

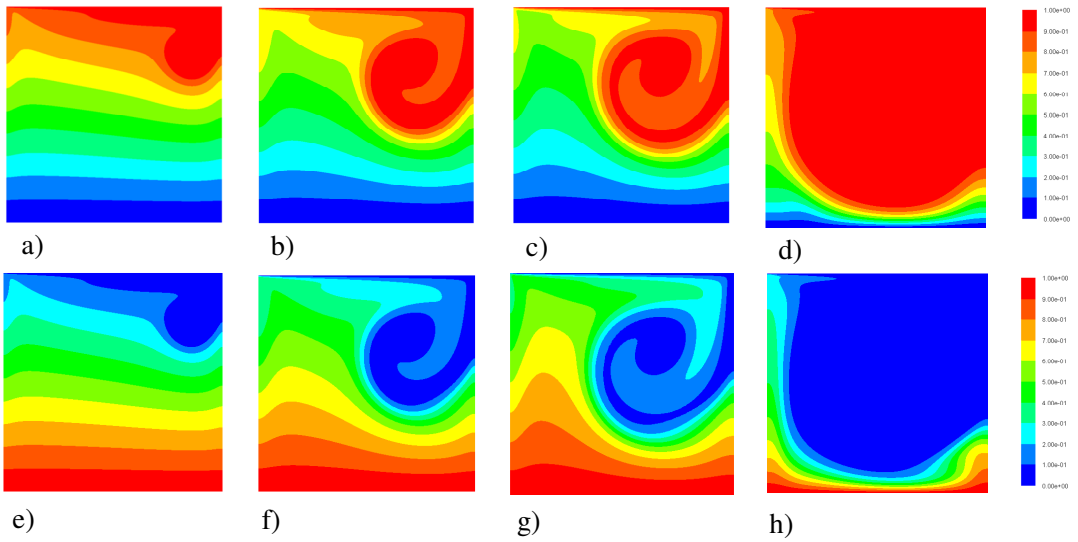

Figure 3. Topologies of the temperature fields for different dimensionless times for $Re_H = 400$, $Ri = 0.1$ and $\Delta T^* = 0.1$. Stable stratification: (a) $t^* = 1.4$; (b) $t^* = 3.7$; (c) $t^* = 5.0$; (d) $t^* = 100.0$ (steady state). Unstable stratification: (e) $t^* = 1.4$; (f) $t^* = 3.7$; (g) $t^* = 5.0$; (h) $t^* = 100.0$ (steady state).

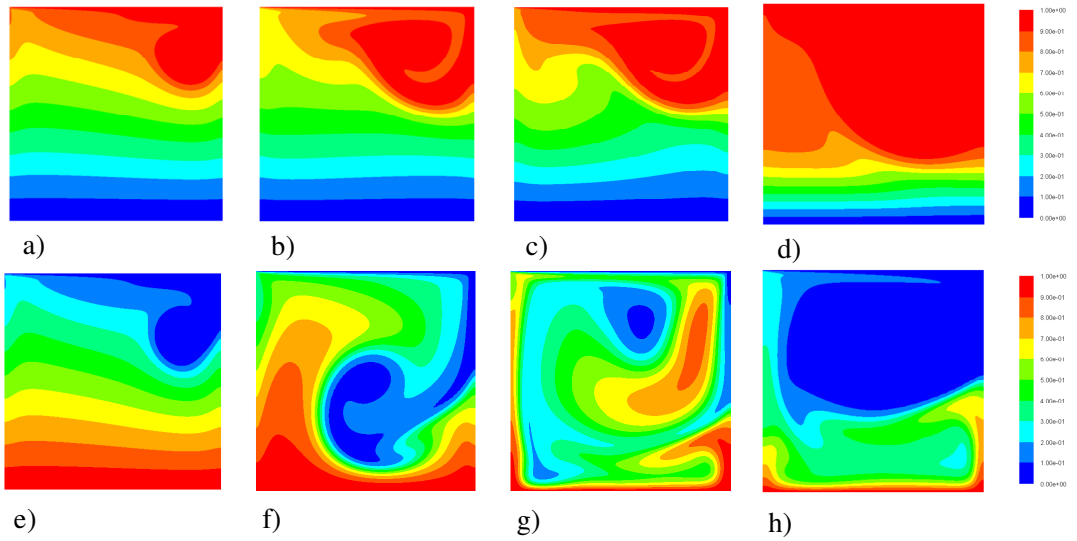

Figure 4. Topologies of the temperature fields for different dimensionless times for Re_H = 400, Ri = 1.0 and $\Delta T^* = 0.1$. Stable stratification: (a) $t^* = 1.8$; (b) $t^* = 4.1$; (c) $t^* = 6.9$; (d) steady state. Unstable stratification: (e) $t^* = 1.8$; (f) $t^* = 4.1$; (g) $t^* = 6.9$; (h) steady state.

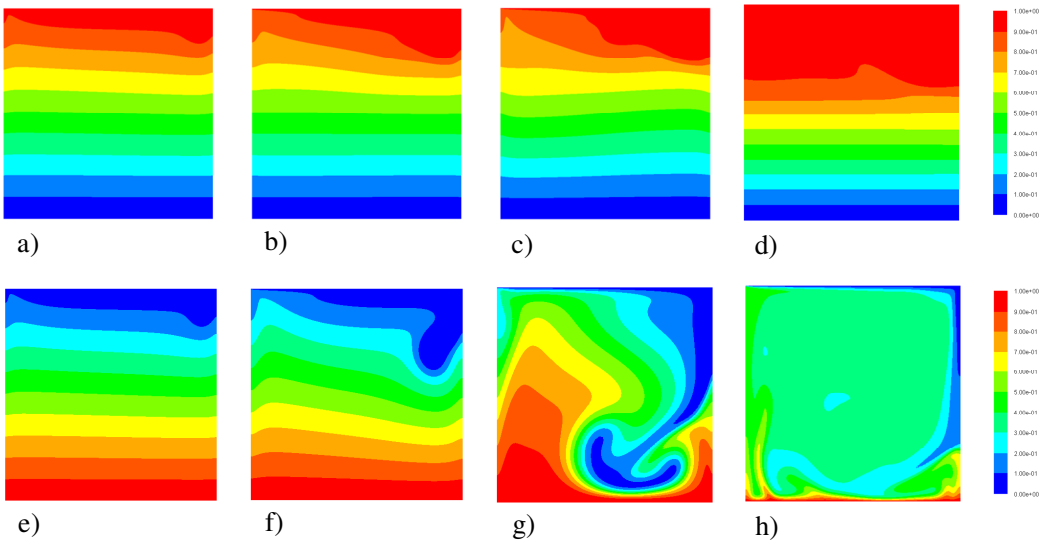

Figure 5. Topologies of the temperature fields for different dimensionless times for Re_H = 400, Ri = 1.0 and $\Delta T^* = 0.1$. Stable stratification: (a) $t^* = 0.5$; (b) $t^* = 1.15$; (c) $t^* = 1.95$; (d) steady state. Unstable stratification: (e) $t^* = 0.5$; (f) $t^* = 1.15$; (g) $t^* = 1.95$; (h) steady state.

For the quantitative analysis of the heat transfer process, it is measured the Nusselt number in the lower and upper surfaces of the cavity. For the lateral surfaces, the Nusselt number is not calculated since the upstream and downstream surfaces are adiabatic. The Nusselt number is given by:

$$Nu_H = \frac{hH}{k} \tag{8}$$

where h is the convective heat transfer coefficient (W/m²K), H is the cavity height (m) which is the characteristic length for the Nusselt number calculations and k is the fluid thermal conductivity (W/mK).

For the numerical simulations, the local Nusselt number is obtained by the measurement of the dimensionless temperature gradient on the analyzed surface, as can be seen in Eq. (9). The space averaged Nusselt number in the lower and upper cavity surfaces is obtained by the spatial integration of the local Nusselt number along the x^* direction, as presented in Eq. (10).

$$Nu_{H,x^*} = \frac{\partial T^*}{\partial y^*} \tag{9}$$

$$\overline{Nu_H} = \int_{x^*=0}^{1} \frac{\partial T^*}{\partial y^*} dx^* \tag{10}$$

Figure 6a and 6b present the local Nusselt numbers on the upper and lower surfaces for stable stratified flows, respectively, when the steady state is reached. In Figure 6a it was observed for all analyzed cases (Ri = 0.1, 1.0 and 10.0) the presence of one peak of the local Nusselt number in the upper surface due to the incidence of a colder mass of fluid on the upper surface by the recirculation. In general, the magnitude of the local Nusselt number was reduced with the increase of the Richardson number, which is in agreement with the previous findings of Iwatsu and Hyun (1995). In Figure 6b it was observed not only differences on the magnitude of Nusselt number but also differences on the behavior of local Nusselt number, which was not noticed on the upper surface. The difference on the local behavior was especially observed when a comparison between the profile for Ri = 0.1 and the profiles obtained with Ri = 1.0 and 10.0 was performed. For the Ri = 0.1 there were a large peak on the local Nusselt number profile for $x^* = 0.6$ due to the influence of the main vortex, which caused a more effective mixing of the fluid in this region. For Ri = 1.0 the local Nusselt number had a slightly variation, reflecting the few oscillations which occurred near the lower surface. For Ri = 10.0 the local Nusselt number was smaller than that for Ri = 0.1 and 1.0 and its behavior was almost constant due to the dominance of diffusion in this region.

Figure 7a and 7b show the local Nusselt numbers on the upper and lower surfaces for unstable stratified flows, respectively, when the steady state is reached. In Figure 7a it was observed the local Nusselt number at the upper surface for the following Richardson numbers: 0.1, 1.0 and 10.0. The behavior of the profiles for the unstable stratification was similar to the ones obtained for the flows with stable stratification. However, the highest Nusselt number was observed for Ri = 10.0, followed by Ri = 1.0 and 0.1, which was exactly the opposite behavior observed for stable stratified flows. In Figure 7b it was observed the local Nusselt number on the lower surface for the following Richardson numbers: 0.1, 1.0 and 10.0. For Ri = 0.1 the behavior of the local Nusselt number for unstable stratified flow was similar to the one previously obtained for the case with stable stratification. For Ri = 1.0, the profile of local Nusselt number for the flow with unstable stratification was quite different from that observed for the case with stable stratification. Two peaks in the local Nusselt number were noticed for the profile with Ri = 1.0, the first one at $x^* = 0.23$ and the second one at $x^* = 0.86$. This behavior was concerned with the generated recirculation in the lower region of the cavity. For Ri = 10.0, the local Nusselt number was higher than those reached for Ri = 0.1 and 1.0, except in the range $1.0 \leq x^* \leq 1.5$ where the local Nusselt number obtained for Ri = 1.0 was higher than that predicted for Ri = 10.0. It is worthy to mention that, for Ri = 10.0, the profile of the Nusselt number had three large peaks and one minor peak. The highest peak happened at $x^* = 0.66$ due to the main vortex and the second and third most intensive peaks ocurred at $x^* = 0.05$ and $x^* = 0.2$, respectively. The second peak happened due to a secondary vortex and the third one was related with a reattachment of a mixture layer in the periphery of the main vortex. The minor peak, noticed at $x^* = 0.95$, is concerned with a secondary flow near the downstream lower corner.

In general, it was observed that, for cavity flows, the increase of the Richardson number lead to the intensification of the mixture between colder and hotter portions of flows, as well as, the arising of more complex fluid dynamic structures such as secondary vortices. This effect was similar to the one observed for forced convection flows when the Reynolds number is increased, i.e., the same ratio between inertial and diffusion forces at forced convection flows can be achieved for mixed convection flows with the aid of buoyancy forces. On the other hand, for stable stratified flows, the buoyancy forces had a similar behavior that those observed for forced cavity flows with decreasing of Reynolds number, i.e., reinforcing the influence of diffusion forces.

Figure 8 presents the space averaged Nusselt number in the lower (or upper) surface for stable and unstable stratified flows with the following Richardson numbers: 0.1, 0.25, 0.5, 0.75, 1.0, 2.5, 5.0, 7.5 and 10.0 at fixed parameters Re_H = 400 and Pr = 6. For the sake of simplicity, only the Richardson numbers of Ri = 0.1, 1.0 and 10.0 were presented for the evaluation of local Nusselt number.

As previously observed, for stable stratified flows the space averaged Nusselt number decreased as the Richardson number increased. The decrease of the Nusselt number was higher in the range $0.1 \leq Ri \leq 1.0$ than for other regions of Richardson numbers, indicating that the effect of stratification was more important for flows where the fluid dynamics and thermal fields were dominated by inertial forces. The difference between the space averaged Nusselt number for Ri = 0.1 and Ri = 1.0 was approximately 63%, while for Ri = 0.1 and Ri = 10.0 this difference increases to 80%. Besides that, for $Ri \geq 5.0$ the space averaged Nusselt number as a function of the Richardson number assumed an asymptotic behavior, showing that the heat transfer process was insensitive for higher Richardson numbers. The percentage difference between the space averaged Nusselt number for Ri = 5.0 and Ri = 10.0 was approximately 5%.

For unstable stratified flows, it was observed a substantial increase in the space averaged Nusselt number for Richardson numbers higher than $Ri \geq 0.75$, i.e., for flows where the fluid dynamic and thermal behavior has a weak

dominance of inertia forces and for flows where there are equilibrium and dominance of buoyancy forces over inertial forces. The percentage variation of the Nusselt number for Ri = 0.1 and Ri = 1.0 was lower than 20%, while the percentage variation for Ri = 0.1 and Ri = 10.0 was approximately 150%. It is worthy to mention a step increase of the Nusselt number from Ri = 0.75 to Ri = 1.0. This fact can be related with modifications of the structure of fluid dynamic and thermal field since it assumed a periodic behavior for Ri = 1.0, which was not observed for flows with Ri ≤ 0.75.

Moreover, it was observed that as the Richardson number increases the difference between the space averaged Nusselt number obtained from the unstable to stable stratified case also increases. The difference for Ri = 0.1 was approximately 14%, while for Ri = 10.0 this difference increased to almost 94%.

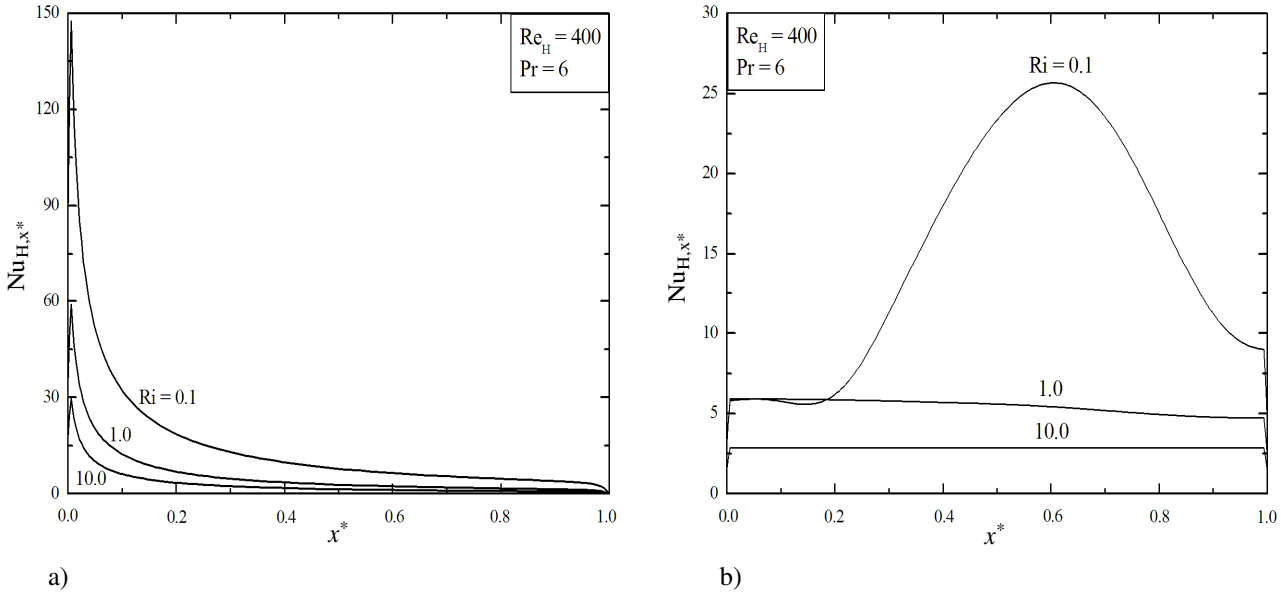

Figure 6. Nusselt number for flows with stable stratification at the steady state: (a) upper surface, (b) lower surface.

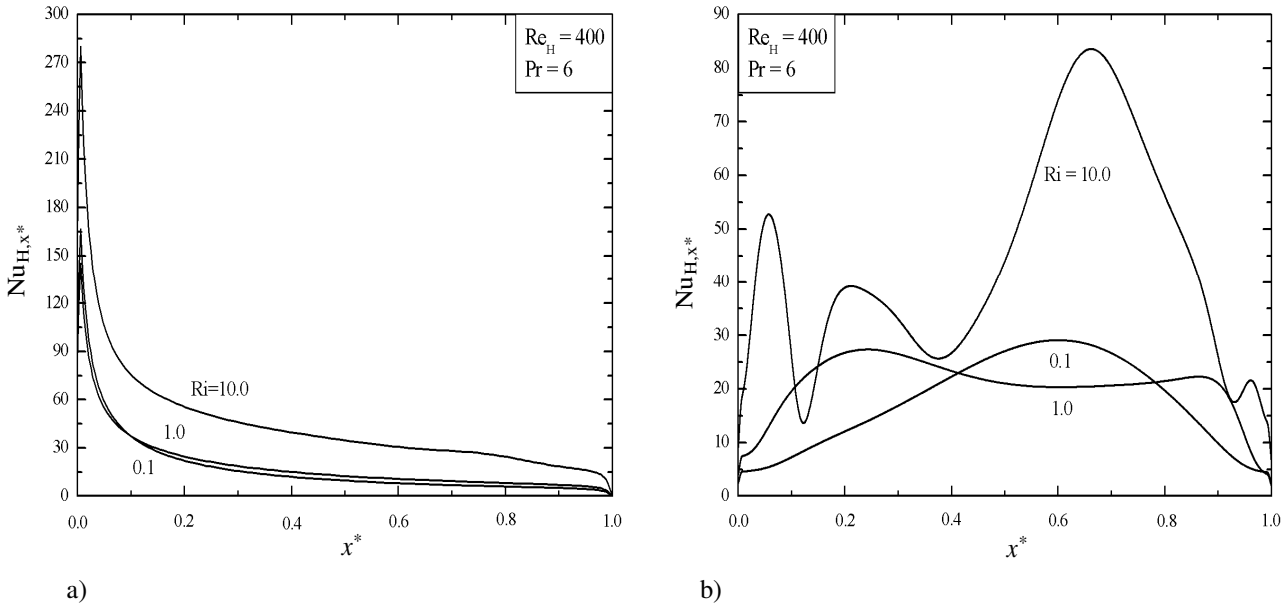

Figure 7. Nusselt number for flows with unstable stratification at the steady state: (a) upper surface, (b) lower surface.

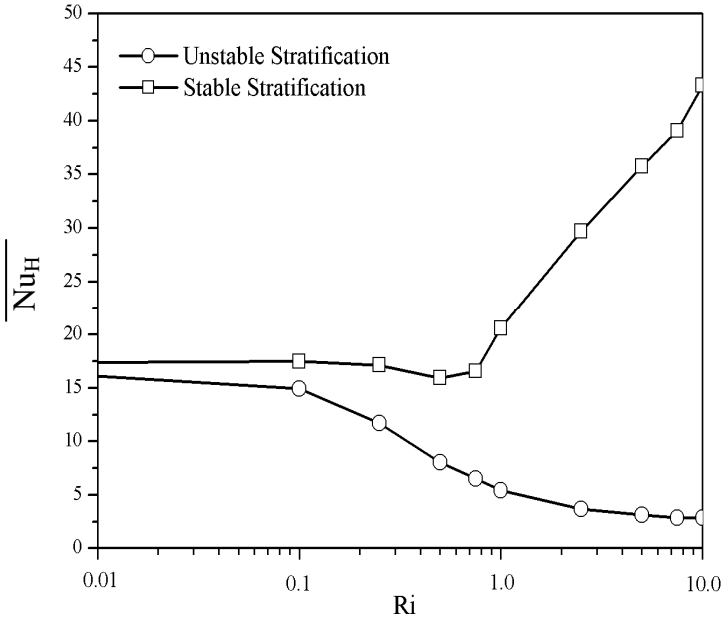

Figure 8. Spatial averaged Nusselt number on the lower surface as a function of Richardson number for stable and unstable stratified flows.

5. CONCLUSIONS

This work presented a numerical study of transient lid-driven cavity flows with mixed convection heat transfer in laminar regime. The influence of the kind of stratification (stable/unstable) over the fluid dynamic and thermal behavior for several Richardson numbers (Ri = 0.0, 0.1, 0.25, 0.5, 0.75, 1.0, 2.5, 5.0 and 10.0) was investigated. For all performed simulations the Reynolds number and Prandtl numbers were kept fixed (Re_H = 400, Pr = 6). The numerical solutions were obtained with a commercial code based on a finite volume method (Fluent, 2007).

The transient temperature topologies for Ri = 0.1, 1.0 and 10.0 showed that the kind of stratification and the variation of the buoyancy forces can affect significantly the transient fluid dynamic and thermal behavior of the flow. For the stable stratified flows, the increase of the buoyancy forces suppressed the heat transfer, especially in the lower region of the cavity flow where the heat transfer occurred almost exclusively by diffusion for Richardson numbers higher than the unity. This behavior was in agreement with the previous findings of Iwatsu and Hyun (1995), Ji *et al.* (2007) and Mohamad and Viskanta (1995). On the contrary, for unstable stratified flows, the increase of buoyancy forces led to the increase of the mixture between hotter and colder regions of the cavity. Besides that, the increase of the Richardson number led to arise of more complex fluid dynamic structures such as secondary vortices, similarly to the effect of Reynolds number increase for forced convection flows.

The local Nusselt number in the lower and upper cavity surfaces were obtained for both kinds of stratification: stable and unstable and for the following Richardson numbers: 0.1, 1.0 and 10.0. For the stable stratified flows the local Nusselt number decreased with the increase of the Richardson number. Moreover, the local Nusselt profile in the lower surface was significantly modified from flows with Ri = 0.1 to Ri = 1.0 and 10.0. For the latter cases, the Nusselt was almost constant, reflecting the diffusively behavior of the heat transfer near the lower surface. On the other hand, for unstable stratified flows, the local Nusselt number was also significantly modified with the increase of the Richardson number. However, in this case the local Nusselt number assumed complex profiles due to the generation of recirculations near the lower surface (Ri = 1.0) and secondary vortices (Ri = 10.0).

To summarize, the space averaged Nusselt number were obtained for both kinds of stratification: stable and unstable, for the following Richardson numbers: 0.0, 0.1, 0.25, 0.5, 0.75, 1.0, 2.5, 5.0, 7.5 and 10.0. For stable stratified flows, the effect of stratification was higher importance for flows where the fluid dynamics and thermal fields are dominated by inertial forces. For unstable stratified flows, the effect of stratification has a higher influence in the heat transfer for flows with Ri $\geq$ 0.75, i.e., for flows where the fluid dynamic and thermal behavior were weakly dominated by inertia towards the dominance of buoyancy forces. Additionally, the increase of the Richardson number increases the difference between the space averaged Nusselt number reached for flows with unstable and stable stratification. The minimum difference, obtained for Ri = 0.1, was approximately 14%, while the maximum difference, for Ri = 10.0, was almost 94%.

6. ACKNOWLEDGMENTS

The second author thanks CAPES by his doctorate scholarship; F. H. R. França thanks CNPq for research grant 304535/2007-9.

7. REFERENCES

Bejan, A., 2004, "Convection Heat Transfer", Wiley, Durhan, USA.

Dos Santos, E.D., Petry, A. P., Rocha, L.A.O, 2008, "Numerical analysis of non-isothermal lid-driven cavity flows using Large Eddy Simulation", Proceedings of the 12th Brazilian Congress of Thermal Engineering and Sciences, ABCM, Belo Horizonte, Brazil.

Dos Santos, E. D., Piccoli, G. L., França, F. H. R., Petry, A. P., 2009, "Numerical Analysis of Transient Convection Heat Transfer Employing Two Different Temporal Schemes: Explicit Iterative of Taylor-Galerkin and Two Step Explicit", Proceedings of 20th International Congress of Mechanical Engineering, ABCM, Gramado, Brazil.

Fluent (version 6.3.16), ANSYS, Inc., 2007.

Guia, U., Ghia, K. N., Shin, C. T., 1982, "High-Re Solutions for Incompressible Flow using the Navier-Stokes Equations and Multigrid Method", J. Comput. Phys., Vol. 48, pp. 387-411.

Iwatsu, R., Hyun, J.M., 1995, "Three-dimensional driven-cavity flows with a vertical temperature gradient", Int. J. Heat Mass Transf., Vol. 38, pp. 3319-3328.

Ji, T. H., Kim, S.Y., Hyun, J.M., 2007, "Transient mixed convection in an enclosure driven by sliding lid", Heat Mass Transf, Vol. 43, pp. 629-638.

Khanafer, K.M., Al-Amiri, A.M., Pop, I., 2007, "Numerical simulation of unsteady mixed convection in a driven cavity using an externally excited sliding lid", Eur. J. Mech. B/Fluids, Vol. 26, pp. 669-687.

Kim, W., Menon, S., 1999, "An Unsteady Incompressible Navier-Stokes Solver for Large Eddy Simulation of Turbulent Flows", Int. J. Numer. Meth. Fluids, Vol. 31, pp. 983-1017.

Maliska, C. R., 2004, "Transferência de Calor e Mecânica dos Fluidos Computacional", LTC.

Mohamad, A.A., Viskanta, R., 1995, "Flow and Heat Transfer in a Lid-driven Cavity Filled with a Stably Stratified Fluid", Appl. Math. Modeling, Vol. 19, pp. 465-472.

Nallasamy, M., Prasad, K. K., 1977, "On Cavity flow at High Reynolds Numbers", J. Fluid Mech., Vol. 79, 391-414.

Patankar, S. V., 1980, "Numerical Heat Transfer and Fluid Flow", McGraw-Hill.

Prasad, A. K., Koseff, J.R., 1989, "Reynolds Number and End-wall Effects on a Lid-driven Cavity Flow", Phys. Fluids A 1, pp. 208-218.

Prasad, A. K., Koseff, J.R., 1996, "Combined Forced and Natural Convection Heat Transfer in a Deep Lid-driven Cavity Flow", Int. J. Heat Fluid Flow, Vol. 17, pp. 460-467.

Versteeg, H. K., Malalasekera, W., 1999, "An Introduction to Computational Fluid Dynamics", Longman.

8. RESPONSIBILITY NOTICE

The authors are the only responsible for the printed material included in this paper.